Localization of brain networks engaged by the sustained attention to response task provides quantitative markers of executive impairment in amyotrophic lateral sclerosis

Roisin McMackin, Stefan Dukic, Emmet Costello, Marta Pinto-Grau, Antonio Fasano, Teresa Buxo, Mark Heverin, Richard Reilly, Muthuraman Muthuraman, Niall Pender, Orla Hardiman, Bahman Nasseroleslami

Angaben zur Veröffentlichung / Publication details:

McMackin, Roisin, Stefan Dukic, Emmet Costello, Marta Pinto-Grau, Antonio Fasano, Teresa Buxo, Mark Heverin, et al. 2020. "Localization of brain networks engaged by the sustained attention to response task provides quantitative markers of executive impairment in amyotrophic lateral sclerosis." *Cerebral Cortex* 30 (9): 4834–46. https://doi.org/10.1093/cercor/bhaa076.

Cerebral Cortex, September 2020;30: 4834–4846

doi: 10.1093/cercor/bhaa076
Advance Access Publication Date: 21 April 2020
Original Article

ORIGINAL ARTICLE

Localization of Brain Networks Engaged by the Sustained Attention to Response Task Provides Quantitative Markers of Executive Impairment in Amyotrophic Lateral Sclerosis

Roisin McMackin[1], Stefan Dukic[1,2], Emmet Costello[1], Marta Pinto-Grau[1,3], Antonio Fasano[1], Teresa Buxo[1], Mark Heverin[1], Richard Reilly[4,5], Muthuraman Muthuraman[6], Niall Pender[1,3], Orla Hardiman[1,7] and Bahman Nasseroleslami[1]

[1]Academic Unit of Neurology, Trinity College Dublin, The University of Dublin, Dublin, D02 R590, Ireland, [2]Department of Neurology, Brain Center Rudolf Magnus, University Medical Center Utrecht, 3584 CX Utrecht, The Netherlands, [3]Beaumont Hospital Dublin, Department of Psychology, Dublin 9, Dublin, Ireland, [4]Trinity College Institute of Neuroscience, Trinity College Dublin, The University of Dublin, Dublin 2, Dublin, Ireland, [5]Trinity Centre for Biomedical Engineering, Trinity College, The University of Dublin, Dublin 2, Dublin, Ireland, [6]Biomedical Statistics and Multimodal Signal Processing Unit, Department of Neurology, Johannes-Gutenberg-University Hospital, D55131, Mainz, Germany and [7]Department of Neurology, Beaumont Hospital Dublin, Dublin 9, Dublin, Ireland

Address correspondence to Orla Hardiman, Academic Unit of Neurology, Trinity College Dublin, The University of Dublin, Room 5.43, Trinity Biomedical Sciences Institute, 152-160 Pearse Street, Dublin D02 R590, Ireland. Email: hardimao@tcd.ie.
Joint Last Authorship: Orla Hardiman (hardimao@tcd.ie) and Bahman Nasseroleslami (bahman.nasseroleslami@tcd.ie)

Abstract

Objective: To identify cortical regions engaged during the sustained attention to response task (SART) and characterize changes in their activity associated with the neurodegenerative condition amyotrophic lateral sclerosis (ALS). Methods: High-density electroencephalography (EEG) was recorded from 33 controls and 23 ALS patients during a SART paradigm. Differences in associated event-related potential peaks were measured for Go and NoGo trials. Sources active during these peaks were localized, and ALS-associated differences were quantified. Results: Go and NoGo N2 and P3 peak sources were localized to the left primary motor cortex, bilateral dorsolateral prefrontal cortex (DLPFC), and lateral posterior parietal cortex (PPC). NoGo trials evoked greater bilateral medial PPC activity during N2 and lesser left insular, PPC and DLPFC activity during P3. Widespread cortical hyperactivity was identified in ALS during P3. Changes in the inferior parietal lobule and insular activity provided very good discrimination (AUROC > 0.75) between patients and controls. Activation of the right precuneus during P3 related to greater executive function in ALS, indicative of a compensatory role. Interpretation: The SART engages numerous frontal and parietal cortical structures. SART–EEG measures correlate with specific cognitive impairments that can be localized to specific structures, aiding in differential diagnosis.

Key words: amyotrophic lateral sclerosis, attention, EEG, hyperactivity, source localization

Introduction

The sustained attention to response task (SART) has been developed to detect clinically relevant lapses in attention. It represents a simple and quantitative task of executive functions that has been used to capture attentional impairments in different neurodegenerative diseases (Robertson et al. 1997; Bellgrove et al. 2006; O'Gráda et al. 2009; Huntley et al. 2017). Drifts in attention are captured by a failure to inhibit motor responses to targets (i.e., commission errors). As the task requires only button press responses, it is suitable for performing during EEG recording with little to no electromyographic artifacts. Recently, SART-generated event-related potentials (ERPs) time-locked to Go and NoGo trials have been interrogated in healthy individuals using quantitative electroencephalography (EEG). These ERPs have individual peaks which relate to sensory detection ("P1" and "N1") (Jin et al. 2019), motor control ("N2"), and attentional engagement ("P3"). The latter two peaks are typically larger during correct response withholding (Zordan et al. 2008). By combining SART with EEG, distinct indices of the neural network activities required for different aspects of task performance can therefore be determined. This facilitates specific interrogation of the sequentially engaged sensory, motor, and cognitive networks on a millisecond-by-millisecond basis in a quantitative, economical manner. Further, by requiring both motor and cognitive performance, the SART is expected to engage networks that bridge cognitive and motor functions, as opposed to tasks that demand only the individual functions. This makes SART a very suitable candidate for interrogating the cortical pathology in neurological conditions which cause both motor and executive decline, including amyotrophic lateral sclerosis (ALS), Huntington's disease, and Parkinson's disease(Gan et al. 2018).

Despite these advantages, the cortical regions engaged by the SART remain unclear. Low-resolution sensor-level topographies have indicated frontoparietal engagement during the task (Zordan et al. 2008; Staub et al. 2015), and dorsolateral prefrontal and anterior cingulate malfunctioning during SART has been reported in Huntington's disease (Beste et al. 2008). However, the sources of the SART ERPs in healthy individuals have yet to be reported in high spatial and temporal resolution.

Such source-resolved measures could provide important insights into and biomarkers of different cognitive and/or motor neurodegenerations, such as occurs in the neurodegenerative condition ALS, for which differential diagnostic markers are urgently required.

ALS is the most common form of motor neuron disease and is characterized by the presence of upper and lower motor neuron degeneration. Clinical (Elamin et al. 2011; Phukan et al. 2012), neuroimaging (Turner et al. 2012), and neuropathological (Gregory et al. 2019) evidence have demonstrated extensive additional nonmotor involvement; however quantitative measurement of this decline in cognition and behavior in ALS remains challenging.

Detailed neuropsychological assessment with appropriate adjustments for motor impairment has provided information on the nature and frequency of different cognitive domain impairments in ALS (Phukan et al. 2012). However, these types of assessments are excessively time-consuming for clinical trials, in some instances are subject to learning effects, and are insensitive to early, presymptomatic network deterioration. Screening tools, such as the Edinburgh cognitive and behavioral screen (ECAS) for ALS, are useful in a clinical setting but have limited utility in clinical trials and are not sufficiently sensitive for a detailed assessment of cognitive/behavioral change (Pinto-Grau et al. 2017). Function magnetic resonance imaging (fMRI) and positron emission tomography (PET) have been used to measure cortical activity during specific tasks, but these technologies are limited by cost (Lulé et al. 2009), low temporal resolution, and variance across different scanners (McMackin et al. 2019c).

By contrast, we and others have recently demonstrated how the source localization of EEG facilitates spatially and temporally precise functional imaging of ALS cortical pathology (Dukic et al. 2019; McMackin et al. 2019a, 2019b). Therefore, given the motor and cognitive pathology of ALS, measurement of SART-associated ERPs using source-resolved EEG provides an opportunity to simultaneously interrogate motor and cognitive network functions and investigate their relationship to symptomatic impairments.

Here, we have spatially resolved the sources of these cognitive indices in healthy individuals and patients with ALS by linearly constrained minimum variance (LCMV)-based source imaging. We demonstrate how quantifying changes in SART–ERP indices and their relation to cognitive and motor symptoms facilitate the investigation of cortical malfunction relating to cognitive impairment in ALS.

Materials and Methods

Ethical Approval

Ethical approval was obtained from the ethics committee of St James's Hospital (REC reference: 2017-02). All participants provided written informed consent before participation. All work was performed in accordance with the Declaration of Helsinki.

Participants

Recruitment

Patients were recruited at the Irish National ALS specialty clinic in Beaumont Hospital. Healthy controls included appropriately consented, neurologically normal, age-matched individuals recruited from an existing population-based control bank.

Inclusion Criteria

Patients were over 18 years of age and diagnosed within the previous 18 months with possible, probable, or definite ALS in accordance with the El Escorial revised diagnostic criteria (Ludolph et al. 2015).

Exclusion Criteria

Exclusion criteria included any diagnosed psychological, neurological, or muscular disease other than ALS, use of CNS medications (e.g., antidepressants, antiseizure medication) except riluzole, inability to participate due to ALS-related motor decline (e.g., inability to sit in the chair for the required time or click the mouse to respond), or evidence of significant respiratory insufficiency. Participants were also rescheduled if they slept two or more hours below normal the night before the session and were asked to abstain from consuming alcohol the night before the recording.

Table 1 Characteristics of ALS patients and controls

	Patients	Controls
n	23	33
Mean age at EEG [range] (years)	63 [32–78]	63.21 [46–82]
Gender (f/m)	3/20	17/16
Site of onset (spinal/bulbar/thoracic)	17/5/1	N/A
Mean disease duration [range] (months)	20.01 [4–42]	N/A
Handedness (right/left/ambidextrous)	22/0/1	31/2/0
C9orf72+	3	Untested
Mean ALSFRS-R score [range]	38.24 [24–43]	N/A
Mean ECAS total score [*n* abnormal]	105.33 [3]	Untested
Mean ECAS ALS-specific score [*n* abnormal]	78.47 [3]	Untested
Mean ECAS ALS-nonspecific score [*n* abnormal]	26.65 [2]	Untested

Handedness was determined by the Edinburgh handedness index. ECAS scores are out of a maximum total score of 136, ALS-nonspecific score of 36, and ALS-specific score of 100. C9orf72+ – carrying a repeat expansion of the C9orf72 gene. ECAS: Edinburgh cognitive and behavioral assessment scale. N abnormal: number of participants scoring below the abnormality cutoff score, accounting for years of education.

Demographics and Characteristics of Patients and Controls

Patient and control characteristics are summarized in Table 1. None of the participants met the criteria for FTD diagnosis. One patient was using noninvasive ventilation at nighttime but was clinically asymptomatic with respect to respiratory impairment and had ALS functional rating scale revised (ALSFRS-R) orthopnea and dyspnea scores of 3 (out of 4).

Experimental Paradigm

Task Design

EEG was recorded across 128-channels during 4×5-min-long consecutive sessions during which participants undertook the SART. Participants were seated 1 ± 0.1 m from a computer monitor where numbers one to nine in single-digit format were appearing in a random order for 250 ms, using Presentation software (Neurobehavioral Systems Inc.). Digits were presented in light gray (RGB code: 250, 250, 250 from 255) on a black background to reduce discomfort associated with the bright light from purely white numbers, reported during protocol testing. Font size was randomized between 100, 120, 140, 160, and 180 points to avoid participants using a perceptual template of the number 3s features for target recognition and to encourage cognitive processing of the numerical value (Robertson et al. 1997). Each stimulus was followed by an interstimulus interval of randomized duration between 1120 and 1220 ms during which time a black screen was presented. Responses were registered by clicking the left button of a computer mouse with the right index finger. Each recording session contained 252 trials of which the number 3 appeared at random in 11% of trials. During these sessions lights were turned off, and experimenters were outside the room to avoid visual/auditory distractions. Online performance and EEG measures were monitored by the experimenter in the neighboring recording room. Appropriate break times were provided to minimize fatigue. Five behavioral measures of performance were captured: NoGo accuracy (percentage of three-digit stimuli followed by response omission), Go accuracy (percentage of nonthree digit stimuli followed by a response in the permitted time window), total accuracy (combined NoGo and Go accuracy), anticipation (clicking less than 150 ms after a go stimulus), and response time.

Participant Instructions

At the beginning of the session, the task was explained to participants using the following instructions: Participants were instructed to click the left mouse button every time they saw a number except for the number 3. Participants were requested to equally prioritize speed and accuracy as both were used as measures of performance. They were asked to refrain from lifting their finger away from the mouse button between clicks as this would increase response time measures. Instructions to use their finger only to click the mouse, avoiding tension in the arm and shoulder, and to reduce noise in the EEG signal were also given. Participants were then given one practice round to ensure they understood the task, which had up to 45 trials (without performance being measured), and it was performed under supervision of the experimenter.

Data Acquisition

EEG Data

EEG recordings were conducted in the Clinical Research Facility at St. James's Hospital, Dublin using a BioSemi ActiveTwo system (BioSemi B.V.) within a room electromagnetically shielded as a Faraday cage. Subjects were measured with an appropriately sized 128-channel EEG cap. Data were online filtered to a bandwidth of 0–134 Hz and digitized at 512 Hz. Participant responses and response time were measured and recorded in individual files as well as being marked on the EEG recording to allow for precise time-locking and categorization of EEG data epochs.

Cognitive and Motor Function Tests

Fifteen patients underwent psychological assessment using the ECAS within 4 weeks of the EEG recording. Additionally, ALSFRS-R was collected longitudinally by neurologists at the Irish national ALS specialty clinic in Beaumont Hospital. Total and ALS-specific ECAS scores within 30 days of EEG data collection were available for 15 patients, while ALS-nonspecific scores were available for 17 patients, and ALSFRS-R scores were available for 14 patients. Three additional patients had ALSFRS-R data within 3 months before and after the EEG recording date. Using the data from these two time points, ALSFRS-R scores for these three patients were estimated by interpolation assuming linear decline such that ALSFRS-R scores were available for 17 patients in total. Scores are summarized in Table 1. Of those patients who performed abnormally in the ECAS, two had abnormal ALS-nonspecific scores but not total or ALS-specific scores, one had an abnormal ALS nonspecific score but could not complete the language, fluency, and spelling tasks to provide remaining scores, and one performed abnormally in total and ALS-specific scores but not in their ALS-nonspecific score.

Data Analysis

Signal Preprocessing

Signal preprocessing was performed using custom MATLAB (R2014a and R2016a, Mathworks Inc.) scripts and the EEGLAB (Delorme and Makeig 2004) and FieldTrip (Oostenveld et al. 2011) toolboxes. Data were filtered using a 0.3-Hz dual-pass fifth-order Butterworth high-pass filter and a 30-Hz dual-pass 117th-order equiripple finite impulse response low-pass filter. Highly contaminated and nonstereotyped artifacts were removed by visual inspection before epoching data from 200 before the stimulus to 900-ms poststimulus. In cases where responses occurred 150 ms or less after stimulus onset, trials were rejected and counted as an "anticipation error." Stereotyped artifacts (e.g., eye blinks, eye movements, and noisy single electrodes) were then removed by independent component analysis (Delorme and Makeig 2004). Data were common average referenced, and mean baseline amplitude was subtracted. Mean correct Go (clicking upon a nonthree digit) and NoGo (not clicking upon a "3" digit), ERPs were calculated for each participant. Due to low error number, there were an insufficient number of clean epochs for incorrect trial-associated ERP analysis. The mean number of included artifact-free correct Go/NoGo trials was 810.13/82.22 for patients and 815.42/82.79 for controls out of a maximum of 897/111.

Sensor Space Analysis

Electrodes of primary interest were chosen based on established topographic maps of the SART N2 and P3 peaks (Zordan et al. 2008; Staub et al. 2015). Four characteristics of the N2 and P3 peaks of each mean Go and NoGo epoch were measured in Fz, FCz, Cz, and Pz electrodes. Namely, the peak (maximal positive amplitude for P3, maximal negative amplitude for N2) amplitude and latency, mean amplitude, and area of the peak within the 220–350-ms and 350–550-ms time windows associated with N2 and P3, respectively. These time windows were chosen based on visual inspection of group mean ERPs and the existing SART–ERP literature (Zordan et al. 2008; Jurgens et al. 2011; Hart et al. 2012, 2015; Kam et al. 2015). Time windows for quantifying peaks of interest were also limited to a maximum of 200 ms to facilitate baseline correction in source analysis (which required matching baseline and peak time windows) while using the same windows for sensor and source analysis.

For assessment of correlations with cognitive performance measures, where similarly significant correlations existed between performance measures and all peak size measures (peak amplitude, mean amplitude, and mean area), we report *P* and rho values with respect to peak amplitude where describing peak size (e.g., "smaller" or "larger").

Source Space Analysis

Channels with continuously noisy data were excluded (excluded channels mean [range] in controls: 0.18 [0–4] and patients: 0.22 [0–4]), and data from these channels were modeled by spline interpolation of neighboring channels. Source localization was performed using custom MATLAB scripts and LCMV beamforming (Van Veen et al. 1997) as implemented in the FieldTrip toolbox. Boundary element head models (Fuchs et al. 2002) incorporating geometries for the brain, skull, and scalp tissues were generated using the ICBM152 MRI template (Fonov et al. 2011), as template-based and individualized boundary element head models are found to provide comparable localization accuracy (Fuchs et al. 2002; Douw et al. 2018).

LCMV was used to estimate brain power maps for the Go and NoGo trails during two time windows, 220–350- and 350–550-ms poststimulus onset, to localize sources of the N2 and P3 ERPs, respectively. Localization was performed of Go and NoGo trials, as well as of the corresponding baseline windows of equal duration (N2: −130 to 0 ms, P3: −200 to 0 ms). Source localizations were performed using common spatial filters (estimated separately for Go and NoGo and for N2 and P3) calculated from epoched data spanning the start of the peak's baseline window to the end of that peak's time window. These common spatial filters were then used to source localize baseline and peak time windows separately. Covariance matrices, used by LCMV, were calculated for individual trials and mean averaged. Regularization of the covariance matrices was implemented at 5% of the average variance of EEG electrodes for each subject separately. Sources within the brain volume were modeled by a grid with 10-mm resolution. The leadfield matrix was normalized to avoid potential norm artifacts (Jonmohamadi et al. 2014). Go and NoGo source activities are reported with baseline correction as $10 \cdot \log_{10}(\text{Power}_{\text{peak}}/\text{Power}_{\text{baseline}})$, with the difference between Go and NoGo source activity reported as $10 \cdot \log_{10}(\text{Power}_{\text{NoGo}}/\text{Power}_{\text{Go}})$.

Statistics

Behavioral Analysis

Group-level comparisons of performance during the SART were implemented with Mann–Whitney *U* test. Adaptive false discovery rate (FDR) of 5% was implemented to correct for multiple comparisons, calculated by the Benjamini–Hochberg method (Benjamini and Hochberg 1995). *P* values are reported as uncorrected values were significant (determined by a corrected value of < 0.05).

Sensor Space Analysis

A four-factor ANOVA was performed for each of the four peak characteristics for both N2 and P3, resulting in eight ANOVA. For each ANOVA the variables included were sex (male or female, accounting for nongender imbalance), trial type (Go or NoGo), electrode (Fz, FCz, Cz, or Pz), and group (ALS patient or control). Post hoc analysis was implemented by Tukey's honestly significant difference (Kim 2015). Adaptive false discovery rate (FDR) of 5% was implemented to correct post hoc *P* values for multiple comparisons as described for behavioral analysis.

Source Space Analysis

A 10-mm grid in the brain volume yields 1726 sources including white matter. To analyze these high-dimensional data, a 10% false discovery rate (Benjamini 2010) was used as a frequentist method for determining significant source activity differences. Discrimination ability between patients and controls is quantified by AUROC (Hajian-Tilaki 2013). Empirical Bayesian inference (Efron 2009) was used to calculate the Bayesian posterior probability and statistical power.

Neuropsychology correlation

Spearman's rank correlation was used to test the association of the changes in EEG measures (peak characteristics or mean power within a cortical region) and cognitive and functional measures based on interindividual differences. These measures

were as follows: Performance in the SART task during EEG collection, performance in the Delis–Kaplan color word interference task (CWIT) (Delis et al. 2004), ECAS scores, and ALSFRS-R scores. Multiple comparison correction was implemented using FDR (Benjamini and Hochberg 1995) set to 5%. For source-level correlation analysis, mean power was calculated for brain regions identified as major sources of peak activity, defined by the Automated Anatomical Labelling atlas (Tzourio-Mazoyer et al. 2002). Where significant correlations are reported regarding Go and NoGo combination measures, for example, total (Go and NoGo) performance accuracy or the difference between NoGo and Go ERP measures, the relationship was verified not to be due to only Go or NoGo trials.

Results

Performance

Patients ($n = 23$) and controls ($n = 33$) did not differ significantly in response time or accuracy. However, patients committed significantly more anticipation errors (patient mean [standard deviation]: 8.73% [13.85%], control mean [standard deviation]: 1.01% [3.26%], $P = 0.0031$).

Control Characteristics

Sensor Space

Mean patient and control Go and NoGo ERPs in electrodes of interest are shown in Figure 1. ANOVAs did not reveal any significant gender effects on waveform features.

N2: N2 in Cz was significantly smaller in Go trials than NoGo trials in controls (peak area $P = 0.018$, peak amplitude $P = 0.006$). This N2 difference significantly correlated with faster response times ($P = 8.08 \times 10^{-6}$, rho = 0.69) and poorer NoGo accuracy ($P = 0.0086$, *rho* = 0.45) in controls (Fig. 2A).

P3: P3 was significantly smaller for Go trials compared with NoGo trials in all four electrodes of interest (Fig. 1, Tukey's post hoc $P = 3.50 \times 10^{-5}$–8.15×10^{-7}). P3 peak latency in the Pz electrodes was also significantly greater in NoGo trials compared with Go trials ($P = 5.12 \times 10^{-7}$). Controls with later responses had later NoGo P3 peaks in Fz ($P = 0.0020$, rho = 0.52), while those with better NoGo accuracy had smaller Go P3 peaks in Cz ($P = 0.011$, rho = −0.43) and FCz ($P = 0.0034$, rho = −0.50), and those with better Go accuracy had larger NoGo P3 peaks in Pz ($P = 0.0070$, rho = 0.46). Better overall accuracy also correlated significantly with smaller NoGo P3 peaks in Fz ($P = 1.26 \times 10^{-4}$, rho = −0.62). Correlations are illustrated in Fig. 3A–D.

Source Space

N2: The left primary motor cortex and bilateral **dorsolateral prefrontal cortex** (DLPFC) and lateral posterior parietal cortex (PPC) were identified as primary mean sources of both Go and NoGo N2, with greater bilateral precuneus activation during NoGo trials (Fig. 4).

P3: Mean P3 sources were similar to those of N2 for Go and NoGo trials, although controls showed decreased left insular, PPC, and DLPFC activity during NoGo trials relative to Go trials (Fig. 5).

ALS Patient Differences

Differences in peak and source measures between patients and controls are summarized in Table 2.

Sensor Space (ERP) Differences

N2: Patients did not show a significant difference in the N2 peak between Go and NoGo trials. Correspondingly, N2 was significantly smaller for NoGo trials in ALS patients compared with controls in FCz ($P = 5.08 \times 10^{-4}$) and Cz ($P = 0.001$). Unlike controls, the difference in N2 between Go and NoGo trials did not correlate with SART performance; however those patients with greater N2 NoGo-Go differences in Cz had higher ECAS total ($P = 0.0022$, rho = −0.73, Fig. 2A) and ALS-specific ($P = 0.017$, rho = −0.61) scores, indicating better cognitive performance, particularly in tasks of executive function and language (Fig. 2B).

P3: The P3 peak did not differ significantly between patients and controls for any trial type or characteristic. Patients and control with longer response times had later ($P = 0.0074$, rho = 0.35), smaller ($P = 2.31 \times 10^{-5}$, rho = −0.53) Go P3 peaks in Cz (Fig. 3E,F). Otherwise, patients did not display the correlations between their P3 peak characteristics and task performance that were observed for controls. Overall accuracy was found to significantly correlate with later Go P3 peaks in Cz in patients ($P = 0.0069$, rho = 0.54, Fig. 3G).

Source Space Differences

N2: Patients showed similar patterns of source activity to controls during N2 (Fig. 4).

P3: While similar locations of source activity were observed in patients and controls during Go and NoGo trials, ALS patients showed similar differences between NoGo and Go source differences to N2 during P3 (Fig. 5), unlike controls. Correspondingly, ALS patients displayed widespread, significantly increased activity during NoGo trials relative to Go trials when compared with controls, with the most discriminant differences (AUROC >0.75) being in the left inferior parietal lobule and left insula (Fig. 6).

Source Space Correlations in ALS Patients

Greater right precuneus power during P3 in NoGo relative to Go trials negatively correlates with CWIT inhibition score ($P = 0.0015$, rho = −0.91, Fig. 7). As greater scores in this task indicated poorer behavioral inhibition, this relationship demonstrated that the abnormal activation of this area was associated with greater preservation of this executive function.

Discussion

This study demonstrates for the first time the specific cortical structures that contribute to performance of the SART and quantifies the relationship between SART performance measures and underlying cognitive performance. Furthermore, we have identified abnormalities in cortical function which strongly correlate with executive impairment in ALS.

ERP Peak Characteristics

At sensor level, our control findings were consistent with the literature, demonstrating the robustness of SART-associated ERPs. N2 and P3 peaks were present in the anticipated time windows and, as expected, larger for healthy individuals during correct response omission.

Central N2

NoGo N2 was maximal in Cz, as previously established. We identified that smaller differences in N2 size between NoGo and Go trials were associated with faster reaction times. We also

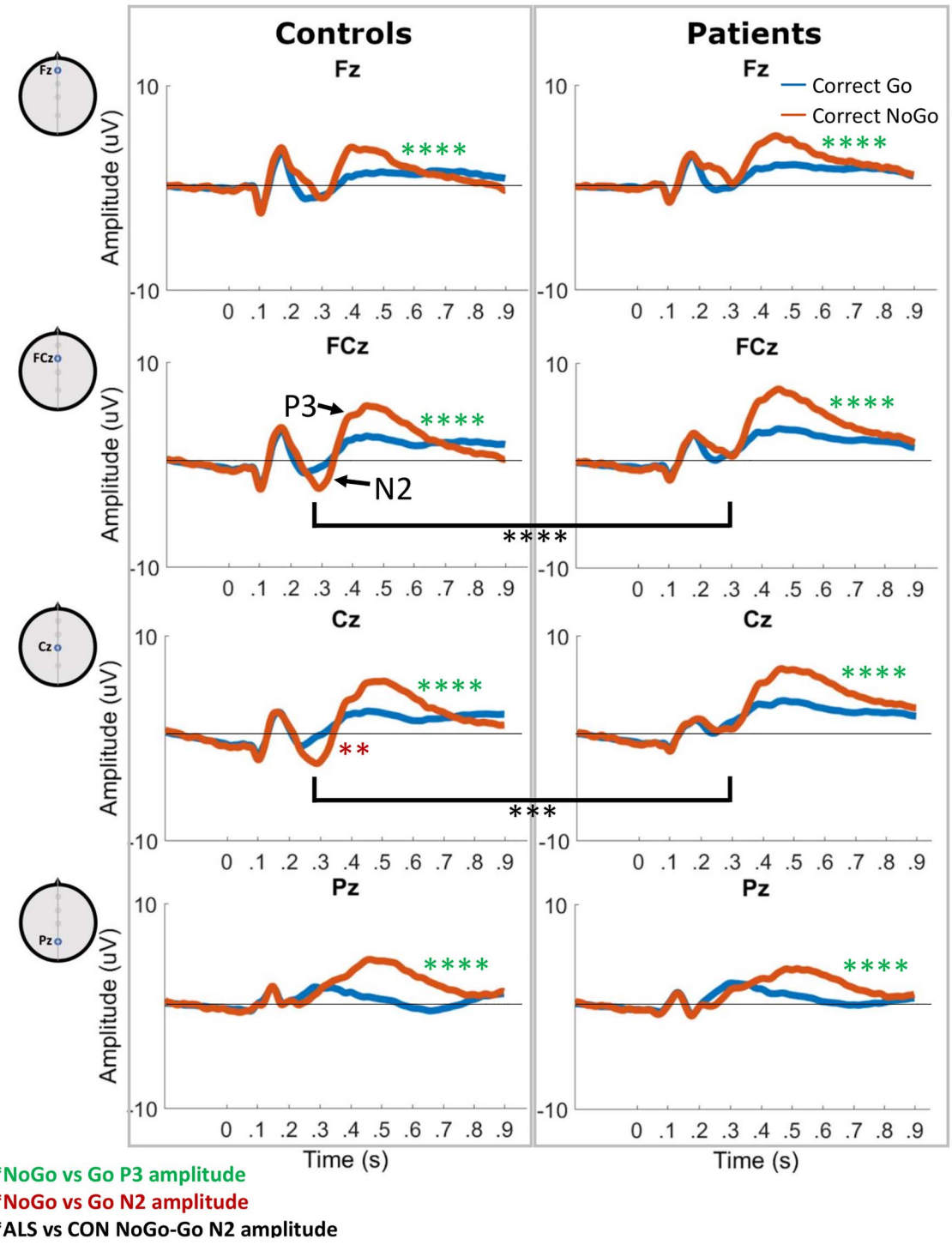

Figure 1. Mean Go (blue) and NoGo (red) trial ERPs in controls and ALS patients. N2 peaks are visible in the NoGo trial ERP in Fz and Cz in the 220–350-ms window. P3 peaks are present in the 350–550-ms window in both Go and NoGo trial ERPs in all electrodes. Green asterisks represent significantly larger P3 peak amplitudes in NoGo versus Go trials. Red asterisks represent significantly larger (more negative) N2 peak amplitudes in NoGo versus Go trials. Black asterisks represent significant differences in NoGo-Go N2 peak amplitude between ALS patients and controls. $^{**}P < 0.01$, $^{****}P < 0.0001$. CON: controls.

identified a correlation between smaller NoGo N2 peaks and better NoGo trial accuracy. As the N2 peak has been associated with automated motor response control (Zordan et al. 2008), this may reflect greater ability to withhold and greater response speed where less cortical resources are required to inhibit upper motor neurons.

Notably, these correlations were not present for ALS patients, which may represent the compensatory engagement of alternative cortical resources. Alternatively, the established malfunction of inhibitory cells of the motor system (Menon et al. 2019) in addition to upper motor neurons may lead to reduction in NoGo N2 in combination with slowing reaction times.

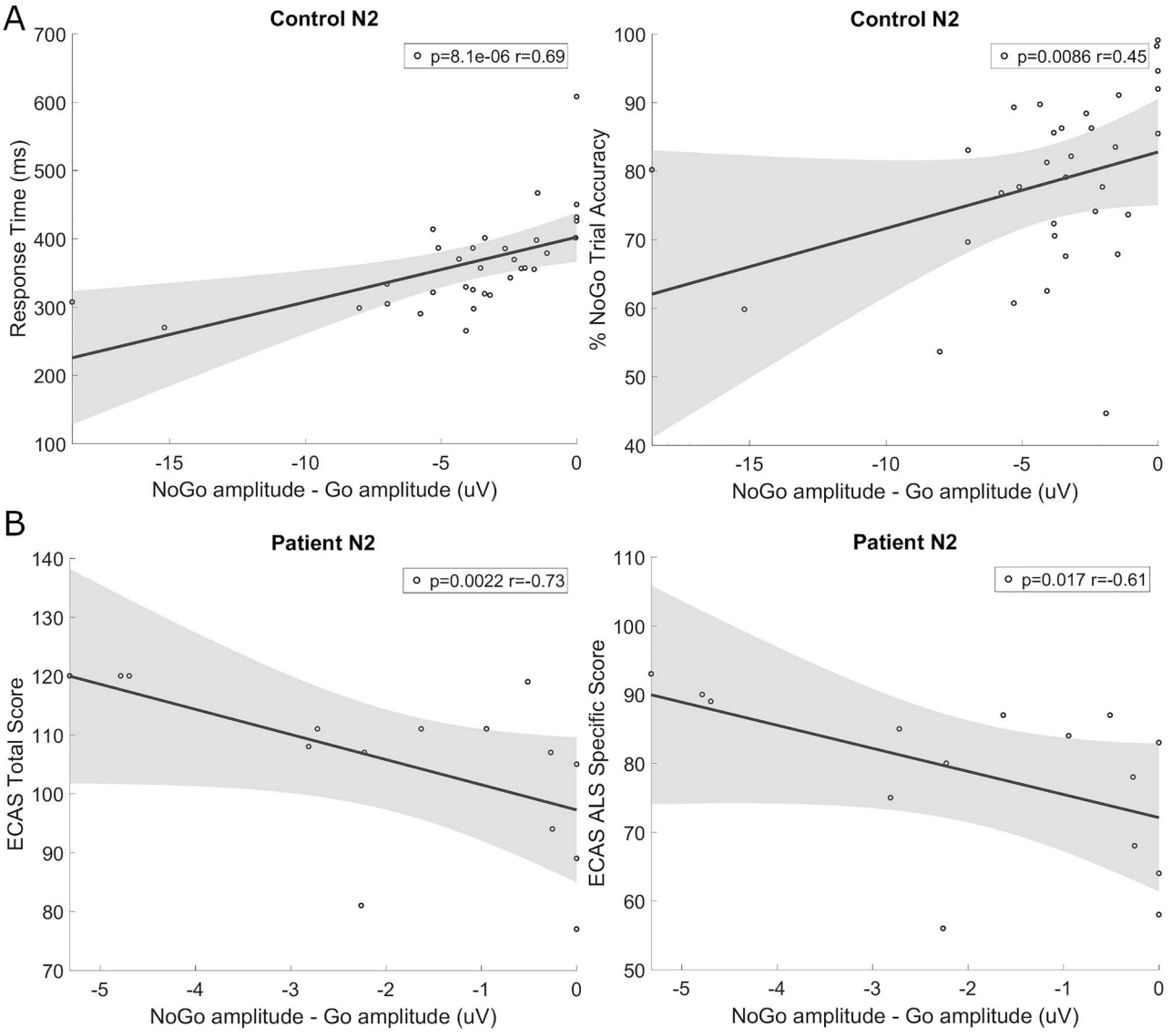

Figure 2. Correlations between NoGo minus Go (NoGo-Go) N2 peak amplitude in Cz and cognitive task performance. (A) Correlation with response time and NoGo trial accuracy in controls demonstrates that those with smaller NoGo versus Go N2 peak differences had significantly faster response times and better NoGo accuracy. (B) Correlation with patient ECAS total and ALS-specific score demonstrates that those with smaller (less negative) N2 peak differences had lower ECAS scores.

Frontal and Parietal P3

The P3 peak was present across the frontoparietal axis of sensors during NoGo trials in keeping with the SART–ERP literature (Zordan et al. 2008; Hart et al. 2012; Staub et al. 2015). Such spatially distributed P3 peaks associated with other cognitive tasks have been shown to consist of two distinct entities, namely, the frontal and parietal P3. Frontal P3 peaks have been associated with orientation to novel stimuli, declining over task duration although remaining elevated in distractible children (Kilpeläinen et al. 1999) and those with panic disorder (Richard Clark et al. 1996). By contrast, parietal P3 peaks are associated with working memory and attention to target stimuli (Richard Clark et al. 1996; Kilpeläinen et al. 1999).

Here we have identified similarly distinct behaviors in the frontal and parietal SART-associated P3 peaks. In frontocentral electrodes, P3 latency related to response timing and is likely to provide an index of orientation speed. Smaller frontocentral P3 peaks were associated with more accurate performance in the opposite trial type (i.e., better Go performance with smaller NoGo peaks and vice versa). By contrast, larger NoGo parietal P3 was associated with better Go trial performance. This is in keeping with the cognitive resources required for accurate Go and NoGo SART performance. The engagement of working memory and attentional control was indicated by a large NoGo parietal P3, and quick orientation to the task was indicated by earlier, smaller frontal P3 peaks (Richard Clark et al. 1996; Kilpeläinen et al. 1999).

The orienting frontal P3 is typically earlier than the parietal P3; however, it has been hypothesized that frontal P3 peaks may also encompass compensatory prefrontal engagement due to parietal decline (van Dinteren et al. 2014). This may explain why ALS patients, but not in controls, demonstrated greater Cz P3 peak latencies during Go trials in those with better accuracy.

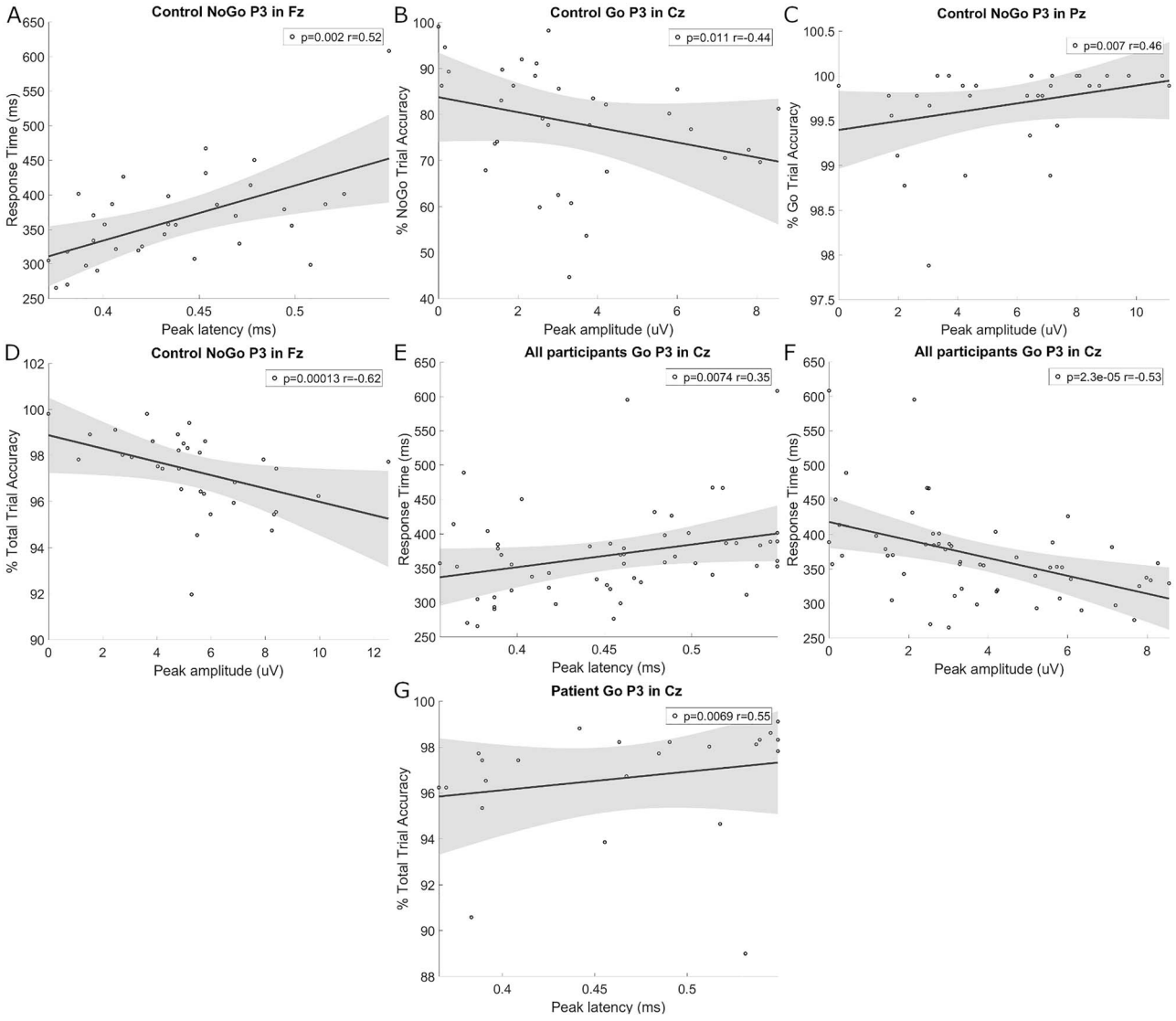

Figure 3. Correlations between P3 peak characteristics and SART performance. In controls, (*A*) later responses correlate with later P3 peaks in Fz during NoGo trials, (*B*) better NoGo accuracy inversely correlates with Go P3 peak size in Cz, (*C*) Go accuracy positively correlates with NoGo P3 peak amplitude in Pz, and (*D*) overall accuracy inversely correlates with NoGo P3 peak amplitude in Fz. In all participants, (*E*) later responses correlate with longer peak latency and (*F*) smaller peak amplitude during Go trials in Cz. In patients, (*G*) greater overall accuracy correlates with longer Go P3 peak latency in Cz.

Cortical Source Imaging

At source level both Go and NoGo N2 and P3 peaks were associated with extensive prefrontal and motor cortex engagement, particularly in the left cortex, in keeping with the use of the right hand for task performance. Such widespread cortical engagement is expected, given the numerous cognitive and motor domains required for accurate task performance. The medial PPC (i.e., the precuneus) was additionally engaged during NoGo trials relative to Go trials during N2, in keeping with its role in both voluntary attention shifting and movement control (Cavanna and Trimble 2006). By contrast, the left insula and inferior parietal lobule show lower power in NoGo trials relative to Go trials during P3, in keeping with the role of the left insula in the salience network (Uddin et al. 2017) and goal-directed behavior (Varjačić et al. 2018). The left inferior parietal lobule has been attributed numerous functions, among which are object-directed action (Chen et al. 2018) and expectancy violation (O'Connor et al. 2010). This engagement of numerous cortical structures by different elements of the SART highlights the range of cortical pathologies that could contribute to decline in SART performance measures. While SART–ERP analysis can temporally dissect the cause of such performance decline, it is clear from source imaging that a specific peak abnormality could also result from dysfunction in several different cortical structures. Source imaging can therefore not only inform on source contributing to cognitive and motor symptoms but could also discriminate between psychiatric or neurodegenerative syndromes with similar symptoms driven by differing cortical pathologies.

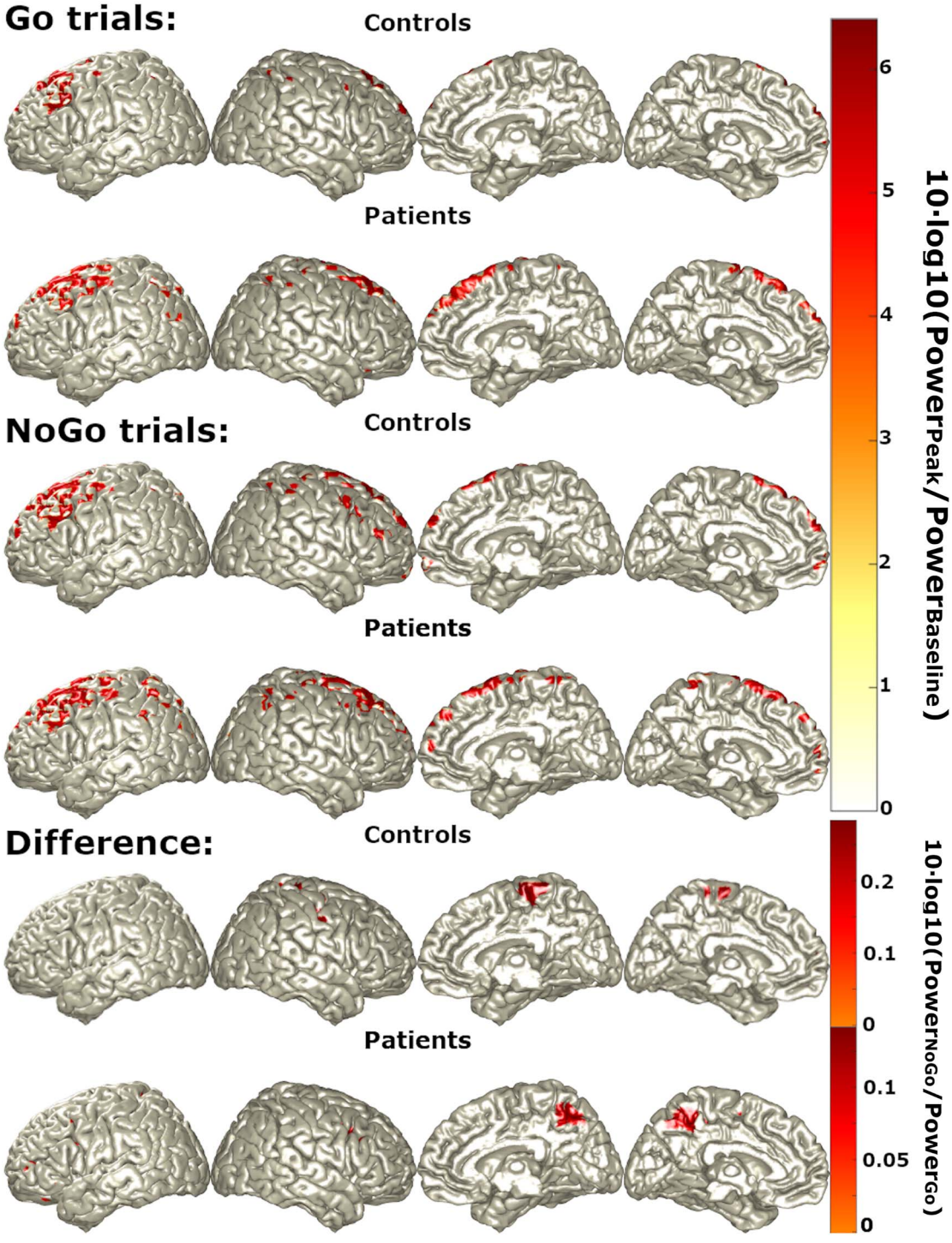

Figure 4. Primary sources (regions with top 5% power) of N2 during Go trials, NoGo trials, and NoGo trials relative to Go trials ("difference") in controls (first rows) and patients (second rows).

Quantifying Cortical Pathology Driving Cognitive Impairment in ALS

ALS patients maintained similar Go and NoGo accuracy but were more likely to attempt to complete trials rapidly clicking before cognitively processing the presented digit, resulting in greater anticipation error. Despite sensor-level differences, patients and control activity did not differ significantly at a specific N2 source. This is likely to be a function of spatially distributed differences in activity which summate in signals captured by individual electrodes at source level. Patients did, however, demonstrate very similar elevation in precuneus activity during NoGo relative to Go trials in both N2 and P3. As this elevation in right precuneus activity during P3 was associated with greater behavioral inhibitory function, this may represent a compensatory recruitment of this region. Indeed, this exemplifies the utility of source

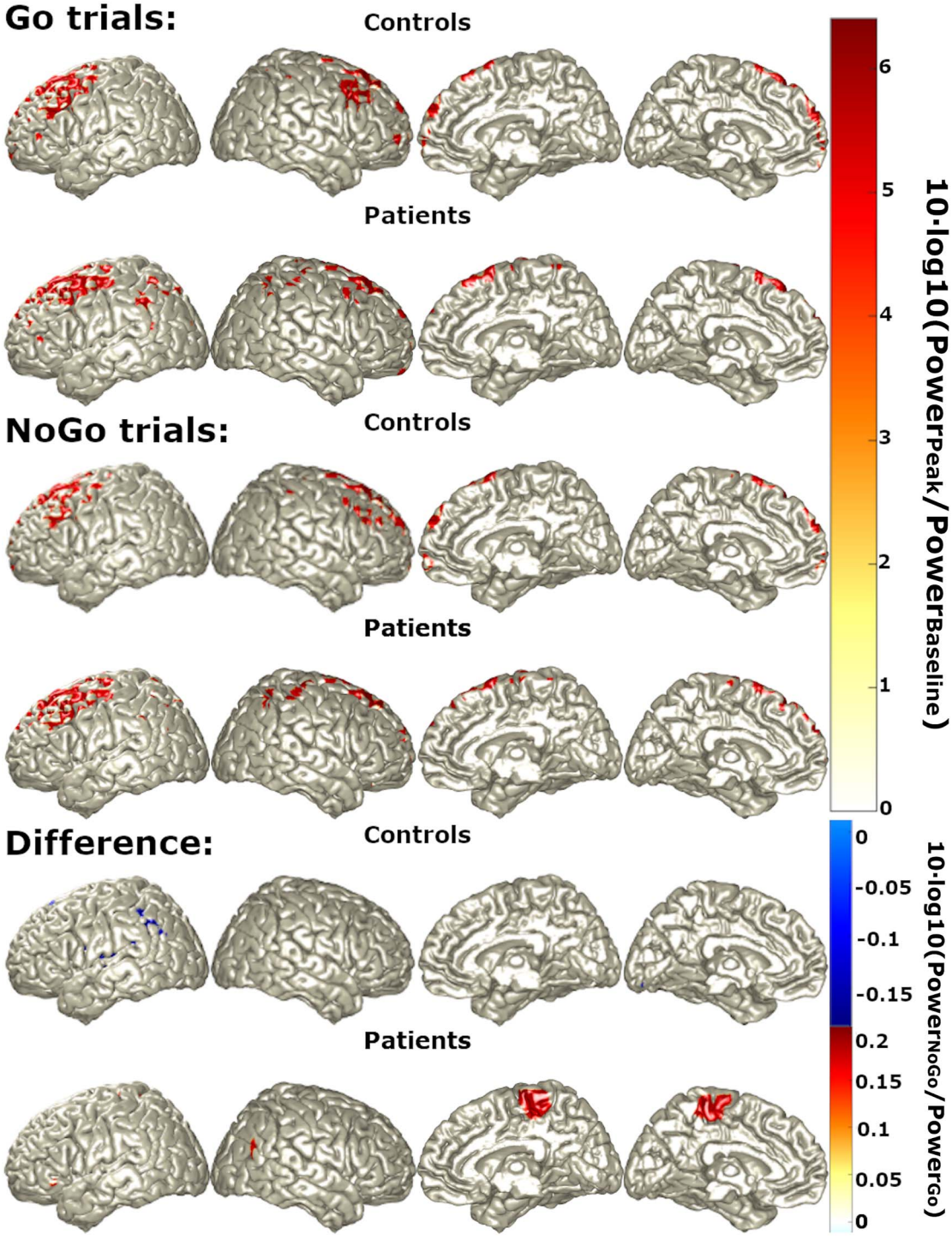

Figure 5. Primary sources (regions with 5% power) of P3 during Go trials, NoGo trials, and NoGo trials relative to Go trials ("difference") in controls (first rows) and patients (second rows).

localized EEG during task performance for quantifying cognitive pathology during presymptomatic phases of compensatory cortical activity that are more amenable to clinical intervention.

ALS patients demonstrated additional widespread cortical activity elevation during NoGo relative to Go trials during P3, particularly in the left insula and inferior parietal lobule, which showed very good discrimination between patients and controls (AUROC > 0.75). Such posterior parietal hyperengagement has previously observed during involuntary attention switching (McMackin et al. 2019b, Dukic et al. 2019) and at rest (Proudfoot et al. 2018; Dukic et al. 2019) and may provide additional discriminatory power in the development of cortical diagnostic

Table 2 Significant differences in ALS sensor-level and source-level measures compared with controls

Sensor level (ERP peaks)			
Peak	Trial	Electrode	Change in ALS
N2	NoGo	Cz	↓ Peak amplitude
		FCz	↓ Peak amplitude
	NoGo-Go	Cz	No correlation to task performance
P3	Go	Cz	Later peak positively correlates with greater overall accuracy, no correlation between peak amplitude and accuracy.
	NoGo	Fz, Pz	No correlation between amplitude or latency to performance
Source level			
Peak	Trial	Source	Change in ALS
P3	NoGo-Go	Left posterior parietal and insular cortex	↑ Activation, area under receivership operating curve > 0.75

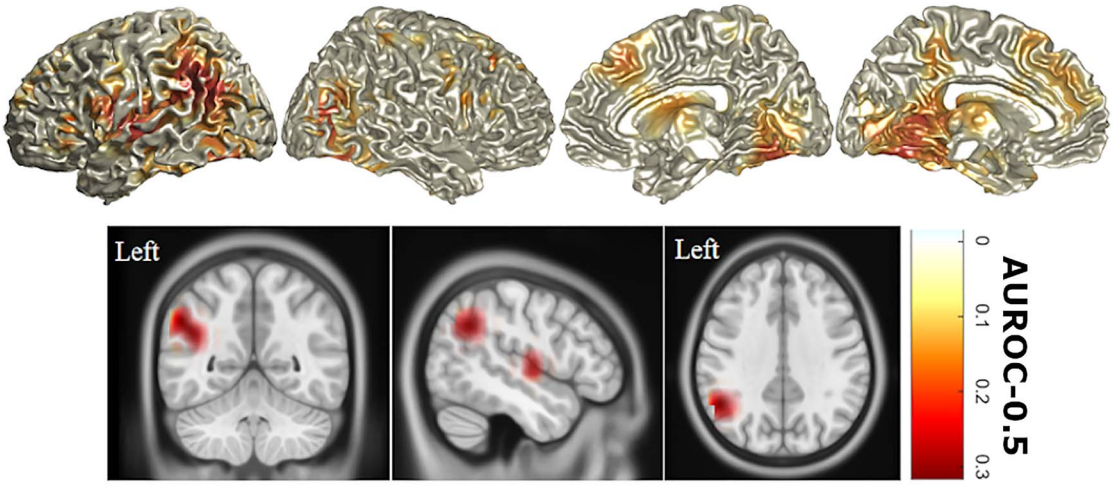

Figure 6. P3 sources with statistically significant differences in activity in ALS compared with controls. Differences between NoGo and Go trial source activity during the P3 peak were compared between ALS patients and controls. All highlighted areas represent significant (FDR = 10%, type II error=0.38 Bayesian Posterior probability=0.87) increases in power with heat map values representing AUROC = –0.5 (i.e., perfect discrimination = 0.5). Orthogonal MRI scans show only those differences with an AUROC >0.75, that is, very good discriminators. AUROC: area under the receivership operating curve.

biomarkers. A previous study in Huntington's disease identified reduced activity in the left DLPFC (Beste et al. 2008), right medial frontal, and anterior cingulate cortex during the NoGo P3, while we find hyperactivity in these areas in ALS, highlighting the ability of this task to identify differing underlying cortical pathologies in neurodegenerations with overlapping cognitive and behavioral symptoms.

We acknowledge that while these cross-sectional data serve well to characterization of ALS disease heterogeneity, these measures demand larger-scale studies for adequately powered subgroup analysis. Additional larger, longitudinal studies will be required to further evaluate the application of this technology in clinical trials and disease prognostics.

In conclusion, here we have provided a spatially and temporally precise description of the cortical activity which underlies the N2 and P3 peaks of the randomized SART–ERP in healthy adults and illustrated the applications of this methodology for interrogating cognitive and motor malfunction in a complex neurodegenerative disease. While larger patient recruitment is required for further investigation of the use of SART as an ALS biomarker, we have established that the SART–ERP and its underlying source activity can provide objective, quantitative, early markers of cognitive and motor pathology. The localization of EEG recorded during a wider battery of cognitive, motor, and sensory tasks has considerable potential to provide patient-specific profiles of cortical network disturbance which could in turn provide biomarkers that improve patient subgrouping, clinical trial stratification, and prognostic accuracy.

Funding

Irish Research Council (grant numbers GOIPG/2017/1014, GOIPD/2015/213); the Health Research Board (grant numbers HRA-POR-2013-246, MRCG-2018-02); Science Foundation Ireland (grant number 16/ERCD/3854); Research Motor Neurone (MRCG-2018-02); and the Thierry Latran Foundation. The psychology aspects of the study were supported by the Motor Neurone Disease Association (grant number Hardiman/Oct15/879-792). MM was supported by Transregional Collaborative Research Center (grant number SFB TR-128) and Boehringer Ingelheim Fonds (grant number BIF-03).

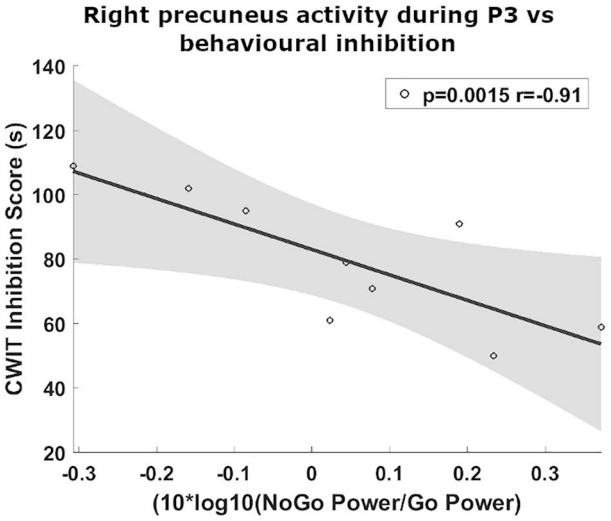

Figure 7. Greater behavioral inhibition in ALS is associated with increased right precuneus activity during NoGo P3 relative to Go P3. Higher CWIT inhibition score indicates poorer behavioral inhibition.

Notes

The authors thank Ms Orla Keenan for her contribution to experimental setup. We thank the Wellcome-HRB Clinical Research Facility at St James's Hospital in providing a dedicated environment for the conduct of high-quality clinical research.

Conflicts of Interest: None declared.

Author Contributions

R.M., B.N., S.D., M.M, N.P., O.H.—conception and design of the study; R.M., S.D.—acquisition and analysis of data; and R.M., S.D., B.N., M.M., O.H.—drafting of manuscript or figures.

References

Bellgrove MA, Hawi Z, Gill M, Robertson IH. 2006. The cognitive genetics of attention deficit hyperactivity disorder (ADHD): sustained attention as a candidate phenotype. *Cortex*. 42 6:838–845.

Benjamini Y. 2010. Discovering the false discovery rate. *Journal of the Royal Statistical Society: series B (Statistical Methodology)*. 72:405–416.

Benjamini Y, Hochberg Y. 1995. Controlling the false discovery rate: a practical and powerful approach to multiple testing. *Journal of the Royal Statistical Society Series B (Methodological)*. 57:289–300.

Beste C, Saft C, Andrich J, Gold R, Falkenstein M. 2008. Response inhibition in Huntington's disease-a study using ERPs and sLORETA. *Neuropsychologia*. 46:1290–1297.

Cavanna AE, Trimble MR. 2006. The precuneus: a review of its functional anatomy and behavioural correlates. *Brain*. 129:564–583.

Chen Q, Garcea FE, Jacobs RA, Mahon BZ. 2018. Abstract representations of object-directed action in the left inferior parietal lobule. *Cerebral Cortex*. 28:2162–2174.

Delis DC, Kramer JH, Kaplan E, Holdnack J. 2004. Reliability and validity of the Delis-Kaplan executive function system: an update. *Journal of the International Neuropsychological Society*. 10:301–303.

Delorme A, Makeig S. 2004. EEGLAB: an open source toolbox for analysis of single-trial EEG dynamics including independent component analysis. *Journal of Neuroscience Methods*. 134:9–21.

Douw L, Nieboer D, Stam CJ, Tewarie P, Hillebrand A. 2018. Consistency of magnetoencephalographic functional connectivity and network reconstruction using a template versus native MRI for co-registration. *Human Brain Mapping*. 39:104–119.

Dukic S, McMackin R, Buxo T, Fasano A, Chipika R, Pinto-Grau M, Costello E, Schuster C, Hammond M, Heverin M, *et al*. 2019. Patterned functional network disruption in amyotrophic lateral sclerosis. *Human Brain Mapping*. 40:4827–4842.

Efron B. 2009. Empirical Bayes estimates for large-scale prediction problems. *Journal of the American Statistical Association*. 104:1015–1028.

Elamin M, Phukan J, Bede P, Jordan N, Byrne S, Pender N, Hardiman O. 2011. Executive dysfunction is a negative prognostic indicator in patients with ALS without dementia. *Neurology*. 76:1263–1269.

Fonov V, Evans AC, Botteron K, Almli CR, McKinstry RC, Collins DL. 2011. Unbiased average age-appropriate atlases for pediatric studies. *Neuroimage*. 54:313–327.

Fuchs M, Kastner J, Wagner M, Hawes S, Ebersole JS. 2002. A standardized boundary element method volume conductor model. *Clinical Neurophysiology*. 113:702–712.

Gan L, Cookson MR, Petrucelli L, La Spada AR. 2018. Converging pathways in neurodegeneration, from genetics to mechanisms. *Nature Neuroscience*. 21:1300–1309.

Gregory JM, McDade K, Bak TH, Pal S, Chandran S, Smith C, Abrahams S. 2019. Executive, language and fluency dysfunction are markers of localised TDP-43 cerebral pathology in non-demented ALS. *Journal of Neurology, Neurosurgery, Psychiatry*.

Hajian-Tilaki K. 2013. Receiver operating characteristic (ROC) curve analysis for medical diagnostic test evaluation. *Caspian Journal of Internal Medicine*. 4:627–635.

Hart EP, Dumas EM, Reijntjes R, Van Der Hiele K, Van Den Bogaard SJA, Middelkoop HAM, Roos RAC, Van Dijk JG. 2012. Deficient sustained attention to response task and P300 characteristics in early Huntington's disease. *Journal of Neurology*. 259:1191–1198.

Hart EP, Dumas EM, van Zwet EW, van der Hiele K, Jurgens CK, Middelkoop HA, van Dijk JG, Roos RA. 2015. Longitudinal pilot-study of sustained attention to response task and P300 in manifest and pre-manifest Huntington's disease. *Journal of Neuropsychology*. 9:10–20.

Huntley JD, Hampshire A, Bor D, Owen AM, Howard RJ. 2017. The importance of sustained attention in early Alzheimer's disease. *International journal of geriatric psychiatry*. 32 8:860–867.

Jin CY, Borst JP, van Vugt MK. 2019. Predicting task-general mind-wandering with EEG. *Cognitive, Affective, & Behavioral Neuroscience*. 19 4:1059–1073.

Jonmohamadi Y, Poudel G, Innes C, Weiss D, Krueger R, Jones R. 2014. Comparison of beamformers for EEG source signal reconstruction. *Biomedical Signal Processing and Control*. 14:175–188.

Jurgens CK, Van Der Hiele K, Reijntjes R, Van De Wiel L, Witjes-Ané MNW, Van Der J, Roos RAC, Middelkoop HAM, van Dijk JG. 2011. Basal ganglia volume is strongly related to P3 event-related potential in premanifest Huntington's disease. *European Journal of Neurology*. 18:1105–1108.

Kam JW, Mickleborough MJ, Eades C, Handy TC. 2015. Migraine and attention to visual events during mind wandering. *Experimental Brain Research*. 233:1503–1510.

Kilpeläinen R, Luoma L, Herrgård E, Yppärilä H, Partanen J, Karhu J. 1999. Persistent frontal P300 brain potential suggests abnormal processing of auditory information in distractible children. *Neuroreport*. 10:3405–3410.

Kim H-Y. 2015. Statistical notes for clinical researchers: post-hoc multiple comparisons. *Restorative Dentistry and Endodontics*. 40:172–176.

Ludolph A, Drory V, Hardiman O, Nakano I, Ravits J, Robberecht W, Shefner J, WFN Research Group On ALS/MND. 2015. A revision of the El Escorial criteria - 2015. *Amyotroph Lateral Sclerosis and Frontotemporal Degeneration*. 16:291–292.

Lulé D, Ludolph AC, Kassubek J. 2009. MRI-based functional neuroimaging in ALS: an update. *Amyotroph Lateral Sclerosis*. 10:258–268.

McMackin R, Bede P, Pender N, Hardiman O, Nasseroleslami B. 2019a. Neurophysiological markers of network dysfunction in neurodegenerative diseases. *Neuroimage Clinical*. 22:101706.

McMackin R, Dukic S, Broderick M, Iyer PM, Pinto-Grau M, Mohr K, Chipika R, Coffey A, Buxo T, Schuster C, *et al*. 2019b. Dysfunction of attention switching networks in amyotrophic lateral sclerosis. *Neuroimage Clinical*. 22:101707.

McMackin R, Muthuraman M, Groppa S, Babiloni C, Taylor J-P, Kiernan MC, Nasseroleslami B, Hardiman O. 2019c. Measuring network disruption in neurodegenerative diseases: new approaches using signal analysis. *Journal of Neurology, Neurosurgery, and Psychiatry*. 90:1011–1020.

Menon P, Yiannikas C, Kiernan MC, Vucic S. 2019. Regional motor cortex dysfunction in amyotrophic lateral sclerosis. *Annals of Clinical and Translational Neurology*. 6:1373–1382.

O'Connor AR, Han S, Dobbins IG. 2010. The inferior parietal lobule and recognition memory: expectancy violation or successful retrieval? *Journal of Neuroscience*. 30:2924–2934.

O'Gráda C, Barry S, McGlade N, Behan C, Haq F, Hayden J, O'Donoghue T, Peel R, Morris D.W, O'Callaghan E, *et al*. 2009. Does the ability to sustain attention underlie symptom severity in schizophrenia? *Schizophrenia research*. 107 (2-3):319–323.

Oostenveld R, Fries P, Maris E, Schoffelen J-M. 2011. FieldTrip: open source software for advanced analysis of MEG, EEG, and invasive electrophysiological data. *Computational Intelligence and Neuroscience*. 2011:1–9.

Phukan J, Elamin M, Bede P, Jordan N, Gallagher L, Byrne S, Lynch C, Pender N, Hardiman O. 2012. The syndrome of cognitive impairment in amyotrophic lateral sclerosis: a population-based study. *Journal of Neurology, Neurosurgery, and Psychiatry*. 83:102–108.

Pinto-Grau M, Burke T, Lonergan K, McHugh C, Mays I, Madden C, Vajda A, Heverin M, Elamin M, Hardiman O, *et al*. 2017. Screening for cognitive dysfunction in ALS: validation of the Edinburgh cognitive and behavioural ALS screen (ECAS) using age and education adjusted normative data. *Amyotroph Lateral Sclerosis Frontotemporal Degeneration*. 18: 99–106.

Proudfoot M, Colclough GL, Quinn A, Wuu J, Talbot K, Benatar M, Nobre AC, Woolrich MW, Turner MR. 2018. Increased cerebral functional connectivity in ALS: a resting-state magnetoencephalography study. *Neurology*. 90:e1418–e1424.

Richard Clark C, McFarlane AC, Weber DL, Battersby M. 1996. Enlarged frontal P300 to stimulus change in panic disorder. *Biological Psychiatry*. 39:845–856.

Robertson IH, Manly T, Andrade J, Baddeley BT, Yiend J. 1997. 'oops!': Performance correlates of everyday attentional failures in traumatic brain injured and normal subjects. *Neuropsychologia*. 35:747–758.

Staub B, Doignon-Camus N, Marques-Carneiro JE, Bacon É, Bonnefond A. 2015. Age-related differences in the use of automatic and controlled processes in a situation of sustained attention. *Neuropsychologia*. 75:607–616.

Turner MR, Agosta F, Bede P, Govind V, Lulé D, Verstraete E. 2012. Neuroimaging in amyotrophic lateral sclerosis. *Biomarkers in Medicine*. 6:319–337.

Tzourio-Mazoyer N, Landeau B, Papathanassiou D, Crivello F, Etard O, Delcroix N, Mazoyer B, Joliot M. 2002. Automated anatomical labeling of activations in SPM using a macroscopic anatomical parcellation of the MNI MRI single-subject brain. *Neuroimage*. 15:273–289.

Uddin LQ, Nomi JS, Hebert-Seropian B, Ghaziri J, Boucher O. 2017. Structure and function of the human insula. *Journal of Clinical Neurophysiology*. 34:300–306.

van Dinteren R, Arns M, Jongsma MLA, Kessels RPC. 2014. Combined frontal and parietal P300 amplitudes indicate compensated cognitive processing across the lifespan. *Frontiers in Aging Neuroscience*. 6:294.

Van Veen BD, van Drongelen W, Yuchtman M, Suzuki A. 1997. Localization of brain electrical activity via linearly constrained minimum variance spatial filtering. *IEEE Transactions on Biomedical Engineering*. 44:867–880.

Varjačić A, Mantini D, Levenstein J, Slavkova ED, Demeyere N, Gillebert CR. 2018. The role of left insula in executive set-switching: lesion evidence from an acute stroke cohort. *Cortex, In Memory of Professor Glyn Humphreys*. 107:92–101.

Zordan L, Sarlo M, Stablum F. 2008. ERP components activated by the "GO!" and "WITHHOLD!" conflict in the random sustained attention to response task. *Brain and Cognition*. 66: 57–64.